Quaternary Research

doi:10.1017/qua.2018.118

Lake-level changes and hominin occupations in the arid Turkana basin during volcanic closure of the Omo River outflows to the Indian Ocean

Xavier Boës[a,b]*, Sandrine Prat[b], Vincent Arrighi[c], Craig Feibel[d,e], Bereket Haileab[f], Jason Lewis[g], Sonia Harmand[g,h]

[a]French National Institute for Preventive Archaeological Research, 12 Rue Louis Maggiorini, 69500 Lyon-Bron, France
[b]CNRS/MNHN/Sorbonne Universités, UMR 7194, Musée de l'Homme, Palais Chaillot, 17 Place du Trocadéro, 75116 Paris Cedex 16, France
[c]French National Institute for Preventive Archaeological Research, 13 rue du Négoce, 31650 Saint-Orens-de-Gameville, France
[d]Department of Earth and Planetary Sciences, Rutgers University, Piscataway, New Jersey 08854, USA
[e]Department of Anthropology and Center for Human Evolutionary Studies, Rutgers University, New Brunswick, New Jersey 08901, USA
[f]Department of Geology, Carleton College, Northfield, MN 55057, USA
[g]Turkana Basin Institute, Stony Brook University, Stony Brook, New York 11794-4364, USA
[h]CNRS, UMR 7055, Préhistoire et Technologie, Université Paris Ouest Nanterre, 21 allée de l'Université, 92023 Nanterre, France

(Received July 12, 2017; Accepted September 13, 2018)

Abstract

In the East African Rift, the western margin of Lake Turkana (northern Kenya) exposes Mio-Plio-Pleistocene lake sediments with dated volcanic horizons constraining basin dynamics at the astronomical time scale. Since the late Pliocene, coastal archaeological sites have formed within the lacustrine dynamics. Here, lake levels are reconstructed from 2.4 to 1.7 Ma using sedimentary facies and water/depth-controlled sediment association. The lacustrine stratigraphy is measured with a total station, and cyclostratigraphy is derived from tephrochronology. The water depths are evaluated from paleochemical properties of lake sediments analyzed by inductively coupled plasma optical emission spectrometry and inductively coupled plasma mass spectrometry. Our reconstruction highlights that Lake Turkana rose during 100 ka insolation/eccentricity maxima periods in response to higher monsoonal inputs of the Omo River. However, Lake Turkana also expanded through an insolation minimum at 2.17–1.95 Ma. This asynchronous lake phase coincides with volcanic closure of the Omo River and Lake Turkana outflow sill to the east and the Indian Ocean. An archaeological hiatus occurs during this endorheic lake phase, and alkalinity increases at the beginning of the hiatus. The lake rose again during insolation/eccentricity maxima at 1.9–1.7 Ma, and a new outflow sill opened to the west and the Nile basin. Hominin coastal occupations return during this exorheic/freshwater lake phase.

Keywords: Early Pleistocene; Lake Turkana; West Turkana; Omo Group deposits; Nachukui Formation; paleolakes; eccentricity; hominin evolution

INTRODUCTION

In East Africa, the role of orbital forcing on climate change in the rift and its implications for hominin evolution remain highly debated (deMenocal, 2004; Ashley, 2007; Trauth et al., 2007; Maslin et al., 2015; Cuthbert et al., 2017; see also Behrensmeyer [2006], Bonnefille [2010], and Levin [2015] for paleoclimate of early human evolution). Over the last decade, paleoclimatic and paleohydrologic hypotheses have been developed not only from distant deep-sea sediment cores (deMenocal, 2004), but also from paleolake exposures much closer to hominin fossil sites (Trauth et al., 2005, 2007, 2010; Deino et al., 2006; Ashley, 2007). In this context, records from several episodes of large, deep lakes have been analyzed from the Plio-Pleistocene in Tanzania, Ethiopia, and Kenya, focusing on the occurrence of diatomites along the East African Rift (Trauth et al., 2005, 2007). These paleolakes would have been relatively synchronous and controlled by periodic arid/humid shifts driven by a ~23 ka precessional insolation cycle. Extreme arid/humid shifts would have occurred every ~400 ka, in response to Earth's eccentricity minima/maxima. Before ~2.7 Ma, extensive deep-water lakes would have been centered on the ~400 ka component of the eccentricity cycle. After ~2.7 Ma, deep paleolakes would have appeared every "~800 ka" only, with periods of precessionally forced extreme arid/humid climate

*Corresponding author at: French National Institute for Preventive Archaeological Research, 12 Rue Louis Maggiorini, 69500 Lyon-Bron, France. E-mail address: xavier.boes@inrap.fr (X. Boës).

variability (Trauth et al., 2007). Thus, recent syntheses linking lake level changes to climate and hominin evolution have proposed the "pulsed climate variability hypothesis" (Maslin et al., 2014, 2015). In this model, a cause-effect relationship is established between extreme arid to humid climate swings and hominin evolution 1.9–1.7 Ma ago, in response to Earth's eccentricity maxima (Maslin et al., 2014, 2015). Applied in the Turkana basin, a key basin for hominin occupations in East Africa, this hypothesis would suggest that Lake Turkana's levels changed in response to extreme climate shifts during the early Pleistocene. However, Lake Turkana is a closed/terminal lake that formed by a succession of major volcanic events that reorganized the Omo River drainage basin at that time (Haileab et al., 2004; Bruhn et al., 2011). Therefore, it could be expected that this lake should respond not only to orbital climate forcing as suggested by Maslin et al. (2014), but also to regional tectono-volcanic activity.

Research objectives

The intent of this article is fourfold: (1) to establish clearly the chronology of lake level changes in the Turkana basin during the early Pleistocene; (2) to reevaluate the role of orbital forcing on lake level changes; (3) to estimate the contribution of tectono-volcanism to a simpler astronomical modulation of the early Pleistocene lake level changes; and (4), after placing the evolution of Lake Turkana into its regional hydrovolcanic context, to discuss the relationships between lake level changes and hominin occupations, with a special emphasis on the evolution of hydrologic conditions.

BACKGROUND

The Turkana basin

The Turkana basin is located within the East African Rift System (EARS) at the junction of two uplifted zones, the Ethiopian dome (>1800 m) and the Kenyan dome (>1000 m; Fig. 1), in the deepest segment of the Kenyan rift (<500 m). This sedimentary basin has accumulated a large amount of lacustrine to volcanic deposits within a series of six half-grabens (Dunkelman et al., 1988) since the formation of the EARS 30 Ma ago (Chorowicz, 2005). The first paleolakes were initiated in the west of the basin during the late Oligocene to early Miocene (Chorowicz, 2005). The Plio-Pleistocene deposits defined as the Omo Group include the Nachukui, Koobi Fora, and Shungura Formations (de Heinzelin, 1983). Of these, the Nachukui Formation on the western side of the basin exposes the most continuous sequence of sediments that are primarily controlled by rift-lake margin dynamics with ~900 m of cumulative strata (Harris et al., 1988; Brown and McDougall, 2011). This sediment package extends from ~4.5 to 0.7 Ma with no major gap, and the chronostratigraphy is constrained by $^{40}Ar/^{39}Ar$ radiometric dating of volcanic tuffs (Harris et al., 1988; Feibel et al., 1989; McDougall and Brown, 2008; Brown and McDougall, 2011; see also McDougall et al. [2012] for the correlations between the volcanic tuffs throughout the Omo-Turkana basin and Brown et al. [1992] for the correlations with tuffs from the Gulf of Aden) and magnetostratigraphic studies (Hillhouse et al., 1977, 1986; Lepre and Kent, 2010; Lepre et al., 2011). Based on the tephrostratigraphy, eight geologic members have been delimited since the 1980s (Harris et al., 1988; see also McDougall et al., 2012): Lonyumun (>4–3.97 Ma), Kataboi (3.97–3.44 Ma), Lomekwi (3.44–2.53 Ma), Lokalalei (2.53–2.33 Ma), Kalochoro (2.33–1.87 Ma), Kaitio (1.87–1.5 Ma), Natoo (1.5–1.3 Ma), and Nariokotome (1.3–0.7 Ma). The Nachukui Formation also includes the Apak (>4.22 Ma), Muruongori (~4 Ma), and Kaiyumung (3.9–3.0 Ma) members (see Feibel, 2003; Brown and McDougall, 2011). The geology of the members expresses large-scale deposits and basin dynamics (Harris et al., 1988).

Hydroclimatic context of Lake Turkana

In the Turkana basin, the Lake Turkana drainage basin (130,000 km^2; Fig. 1) occupies two very contrasted hydroclimatic zones: the arid-hot Turkana lowlands (<500 meters above sea level [m asl]; <300 mm/yr of precipitation; mean annual temperature of 30°C; Lien et al., 1988) and the tropical-humid Ethiopian highlands (>1500 m asl; >1500 mm/yr of precipitation; mean annual temperature of 19°C; Olaka et al., 2010). In contrast to the tropical monsoonal climate in the Ethiopian highlands, the Turkana lowlands have a desert climate according to the Köppen classification (550 $cal/cm^2/d$; Peel et al., 2007). The Turkana lowlands have been constantly arid during the past 4 million yr (Passey et al., 2010). The regional aridity was initiated ~10 Ma ago, since tectonic uplift of East Africa created a topographic barrier for atmospheric circulation and precipitation (Sepulchre et al., 2006). In this orographic context, the low-level Turkana jet produces patterns of descending air that enhance aridity in the Turkana depression (orographic channeling effect; Nicholson, 2016).

Although Lake Turkana is located within the arid-hot Turkana closed depression, it is the largest lake (7500 km^2) in an arid environment on the planet (Bloszies and Forman, 2015). The lake is 260 km long but averages only 30 m depth, with a maximum of 110 m. Today, Lake Turkana is terminal/endorheic with no outflow to the Indian Ocean or Mediterranean Sea (via the Nile basin). Thus, the existence of this large closed interior basin lake depends almost completely on inflows from the tropical Ethiopian highlands: 80% to 90% of freshwater inflow is supplied by the perennial Omo River. The other main tributaries are the intermittent Turkwel and Kerio Rivers (southern basin; Fig. 1), which provide the other 10% to 20% (Bloszies and Forman, 2015). If the drainage basin was restricted to the Turkwel and Kerio, there would be no permanent lake in the arid Turkana depression. Because the Omo River drainage basin ends in Lake Turkana today, the modern lake equilibrates between freshwater

https://doi.org/10.1017/qua.2018.118 Published online by Cambridge University Press

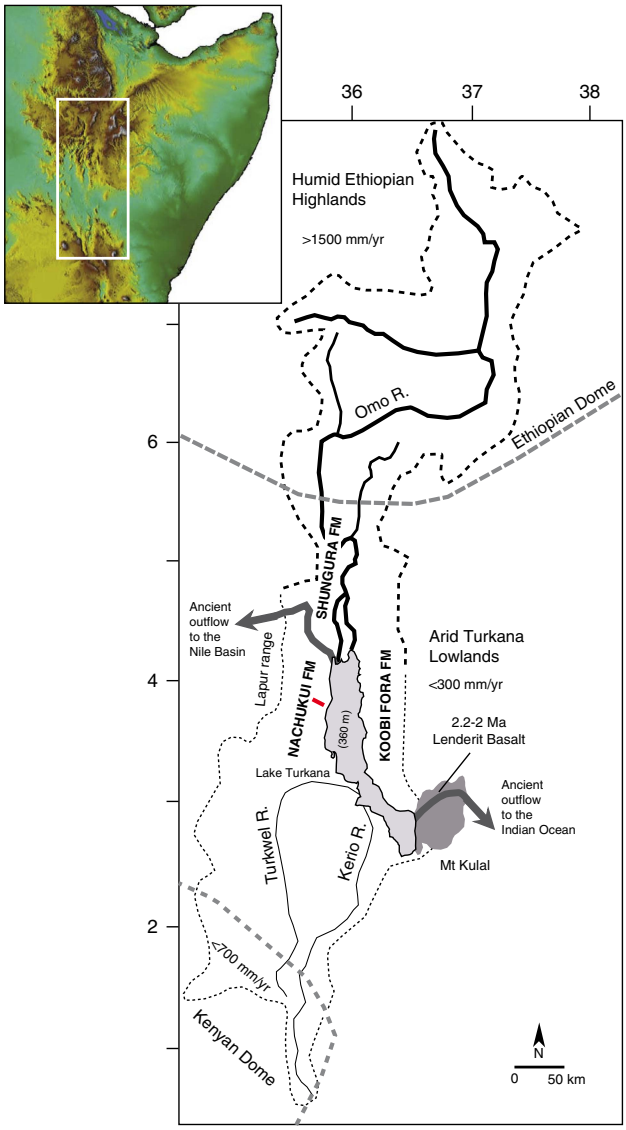

Figure 1. (color online) Map of the Omo-Turkana drainage basin (dashed lines) showing the location of the geologic cross section (red bar) for the stratigraphic interval between 2.4 and 1.72 Ma presented in Figures 2 and 3. The drainage boundaries and elevation were calculated from Global Multi-resolution Terrain Elevation Data 2010 (GMTED2010; Danielson and Gesch, 2011).

inputs from the Omo River (<500 m^3/s, Lien et al., 1988) and evaporation outputs (2.5–3.5 m/yr; Lien et al., 1988). The lake water is therefore currently alkaline (21–34 meq/L; Lien et al., 1988; Olago and Odada, 1996; see also Cerling, 1979), with a moderate salinity/Total Dissolved Solids (2500 ppm; Yuretich and Cerling, 1983).

Turkana paleolakes

Paleolakes have fluctuated up to +100 m above the modern level (360 m asl), providing evidence for hydrologic history that is exceptional for East Africa (Halfman, 1987; Olaka et al., 2010; Garcin et al., 2012). On the western margin of the Turkana basin, stratigraphic evidence of lake fluctuations is found within the Nachukui Formation at: >4–3.99 Ma (Lonyumun Lake phase; Feibel, 2011); ~3.5 to 3.3 Ma (Lokochot Lake phase; Feibel, 2011); ~3.15 Ma (Waru Lake phase; Feibel, 2011); ~2.5 Ma (Lokeridede Lake phase; Feibel, 1997); 2.4 to 2.3 Ma (Kokiselei Lake phase; this study); 2.25–2.2 Ma (Nasura Lake phase; this study); 2.17 to ~1.95 Ma (pre–Lorenyang Lake phase; this study); ~1.95 to ~1.76 Ma (Lorenyang Lake phase; this study); ~1.1–0.9 Ma (Silbo Lake phase; Feibel, 1997). Most of the depositional environments in west Turkana appear to be related to these paleolake systems, and very few are fluvial and terrestrial sensu stricto; some lacustrine carbonates became "pedogenic" following exposure. In the rift axis, paleolake levels (paleoshorelines) are deformed by tectonics, but paleolake fluctuations are well expressed by the stratigraphic sequences of offshore, shoreface, beachface, and backshore systems (see Nutz et al., 2017; Schuster and Nutz, 2018).

Volcanic closure of Lake Turkana

Tectonics and volcanism have played an important role in the reorganization of Paleolake Turkana and paleo–Omo River outflow systems (see Haileab et al., 2004; Gathogo et al., 2008; Opdyke et al., 2010; Bruhn et al., 2011). Before 4.5 Ma, the Omo-Turkana drainage system had a northern outlet channel to the west and the Mediterranean Sea (Haileab et al., 2004; Bruhn et al., 2011). This outlet channel was cut off by subsidence and the formation of a lower southeastern outflow sill to the Indian Ocean (the Hoi channel; see Bruhn et al., 2011). After 3.95 Ma, the southeastern outlet channel was probably relocated north of Loiyangalani (southeastern end of the lake) because of the eruptions of the Gombe Basalts at 4.5–3.95 Ma (Bruhn et al., 2011). From 2.5 to 2 Ma, successive channel outlet routes formed between the southeastern end of the lake and the entrance to the modern Chalbi desert. Outflows to the Indian Ocean were finally cut off by several eruptions of lava flows (Lenderit, Marsabit, and Balo; Fig. 1) from 2.2 to 1.8 Ma (Haileab et al., 2004; Bruhn et al., 2011). Since the final closure of the southern route to the Indian Ocean, outflows to the Nile basin were temporarily open thereafter (e.g., during the African Humid Period lake high stand; Garcin et al., 2012).

Hominin coastal occupations

In the western side of Lake Turkana, the Nachukui Formation is a key field survey area because it exposes nearly continuous stratigraphic sequences of paleolake margin deposits along with numerous associated archaeological sites from the late Pliocene and early Pleistocene (Kibunjia et al., 1992; Kibunjia, 1994; Roche et al., 1999, 2003; Prat et al., 2003, 2005; Tiercelin et al., 2010; Harmand et al., 2015). Despite the Nachukui Formation deposits being mostly related to subaqueous environments, the number of archaeological sites is high (Roche et al., 2003) because of a cumulative effect of hominin occupations along shifting shorelines, which also

https://doi.org/10.1017/qua.2018.118 Published online by Cambridge University Press

favored site formation processes through time (for the geologic context, see Roche et al., 1999, 2003; Prat et al., 2003, 2005; Tiercelin et al., 2010; Harmand et al., 2015). Thus, this region is an important piece of the puzzle in terms of hominin behavioral evolution: the earliest known knapped stone artifacts are found at 3.3 Ma at Lomekwi 3 (Harmand et al., 2015; Lewis and Harmand, 2016), early Oldowan stone artifacts are found at Lokalalei 1 and 2C at 2.34 Ma (Kibunjia, 1994; Roche et al., 1999; Delagnes and Roche, 2005), and the earliest known Acheulean bifaces occur at Kokiselei 4 at 1.76 Ma (Lepre et al., 2011).

The Nachukui Formation also provides the highest number of hominin species from the Omo Group, shedding light on key questions for human evolution and dispersal (e.g., Brown et al., 1985; Walker et al., 1986; Brown and Feibel, 1988; Leakey and Walker, 1988; Walker and Leakey, 1993; Brown et al., 2001; Leakey et al., 2001; Prat et al., 2005). Indeed, several fossil discoveries made in West Turkana have changed previous phylogenies and ideas about hominin evolution (*Australopithecus*, *Paranthropus*, and early *Homo* lineages; see, e.g., Wood and Constantino, 2007; Wood and Leakey, 2011; see also Feibel et al. [1989] for the stratigraphic context of fossils). We can mention, for example, the specimens KNM-WT 40000 (*Kenyanthropus platyops*; 3.5–3.2 Ma; Leakey et al., 2001), KNM-WT 17000 (*Paranthropus aethiopicus*; 2.5 Ma; Walker et al., 1986), KNM-WT 42718 (early *Homo*; 2.4–2.3 Ma; Prat et al., 2005), and KNM-WT 15000 (*Homo erectus/ergaster*; 1.6–1.5 Ma; Walker and Leakey, 1993). Comparatively, the ~2.5–2 Ma key interval in hominin evolution is not well exposed/preserved in the Koobi Fora Formation on the eastern side of the basin.

MATERIAL AND METHODS

Site location

Because of the time period of interest (early Pleistocene evolution of Lake Turkana), we have concentrated our field surveys on the Kalochoro Member of the Nachukui Formation (2.33–1.87 Ma). The upper Lokalalei Member has also been surveyed to extend our reconstruction up to 2.4 Ma, as well as the lower Kaitio Member, for the stratigraphic interval between 1.87 and ~1.7 Ma. This stratigraphic interval includes four volcanic tephra that have been identified and radiometrically dated since the 1980s (Harris et al., 1988; Feibel et al., 1989; McDougall and Brown, 2008; Brown and McDougall, 2011; McDougall et al., 2012): the Kokiselei Tuff (2.4 ± 0.05 Ma) is exposed at the top of the Lokalalei Member; the Kalochoro Tuff (2.33 ± 0.02 Ma) and Tuff G (2.27 Ma ± 0.04 Ma) are exposed at the base of the Kalochoro Member; and the KBS (Kay Behrensmeyer Tuff) Tuff (1.87 ± 0.02 Ma) is found at the base of the Kaitio Member. In this tephrostratigraphic context, two Oldowan archaeological site complexes, Kokiselei and Nasura (Roche et al., 2003; Harmand et al., manuscript in preparation), have been intensively surveyed and excavated between 2010 and 2017 by the West Turkana Archaeological Project (WTAP).

Geologic survey

Following the geologic members, we have established a geologic section across the upper Lokalalei, Kalochoro, and lower Kaitio Members (Figs. 2, 3). The geologic section begins with the Kokiselei Tuff at an elevation of 417 m and ends at 442 m. Stratigraphically, the section ends ~15 m below the KBS bentonite that delimits the Kalochoro/Kaitio Member boundary. For the stratigraphic interval of 15 m below and 24 m above the KBS, our cross section is completed by that of Nutz et al. (2017), which has been established in the continuation of our section up to 463 m. The stratigraphic interval of 15 m below the KBS is characterized by offshore muds, and the sediments 24 m above are mostly marked by shoreface oncolite-rich silty-sands from the end of Lorenyang Lake phase (see Nutz et al., 2017). The geologic section can be observed along the Kokiselei ephemeral stream (base: 4°0.197′N, 35°47.946′E; top: 4°0.387′N, 35°46.863′E; WGS84). The top of the section from Nutz et al. (2017) is located at the Kokiselei locality (top: 4°0.307′N, 35°46.518′E; WGS84).

Total station survey

The method applied to carry out the geologic cross section is the routing method supported by the method of radiation with a total station (measure angle and distance to each feature; X, Y, Z of the surveyed points, Leica TS06 total station). The routing is represented in the plan as a broken polygonal line in which the mutual position of the points is determined by measuring the distances between the breaking points and by measuring the angles in the breaking points of the polygonal route. The routing supposes the increase of the geodesic network to determine the detail point coordinates in the field. The increase of the geodesic network was done by determining the coordinates of some points that become the main elements of the topographic survey. The main elements are volcanic beds and lake sediment successions. A paleolake phase is defined as a conformable succession of genetically related beds, including sand and pebbles (high-energy fluviolacustrine deposits; flooding surface); sands (high-energy deposits/foreshore system); sands and shells (high-energy waves deposits/beachface system; see Nutz et al., 2017; Schuster and Nutz, 2018); homogeneous clays (very low-energy lake deposits/offshore system); bioturbated silts with wave ripple laminations (low-energy lake deposits/lower shoreface system); cross-bedded silts to medium sand (low- to high-energy lake deposits/upper shoreface system). The bottom and top of each system have been measured with the total station (Fig. 2).

Geochronology

The geochronology is established using the projection of the volcanic tuffs in the stratigraphy as measured by the total station (Figs. 3, 4). The volcanic tuffs were located and sampled, and their GPS coordinates were compared to samples analyzed and identified by Haileab (1995) at the same

https://doi.org/10.1017/qua.2018.118 Published online by Cambridge University Press

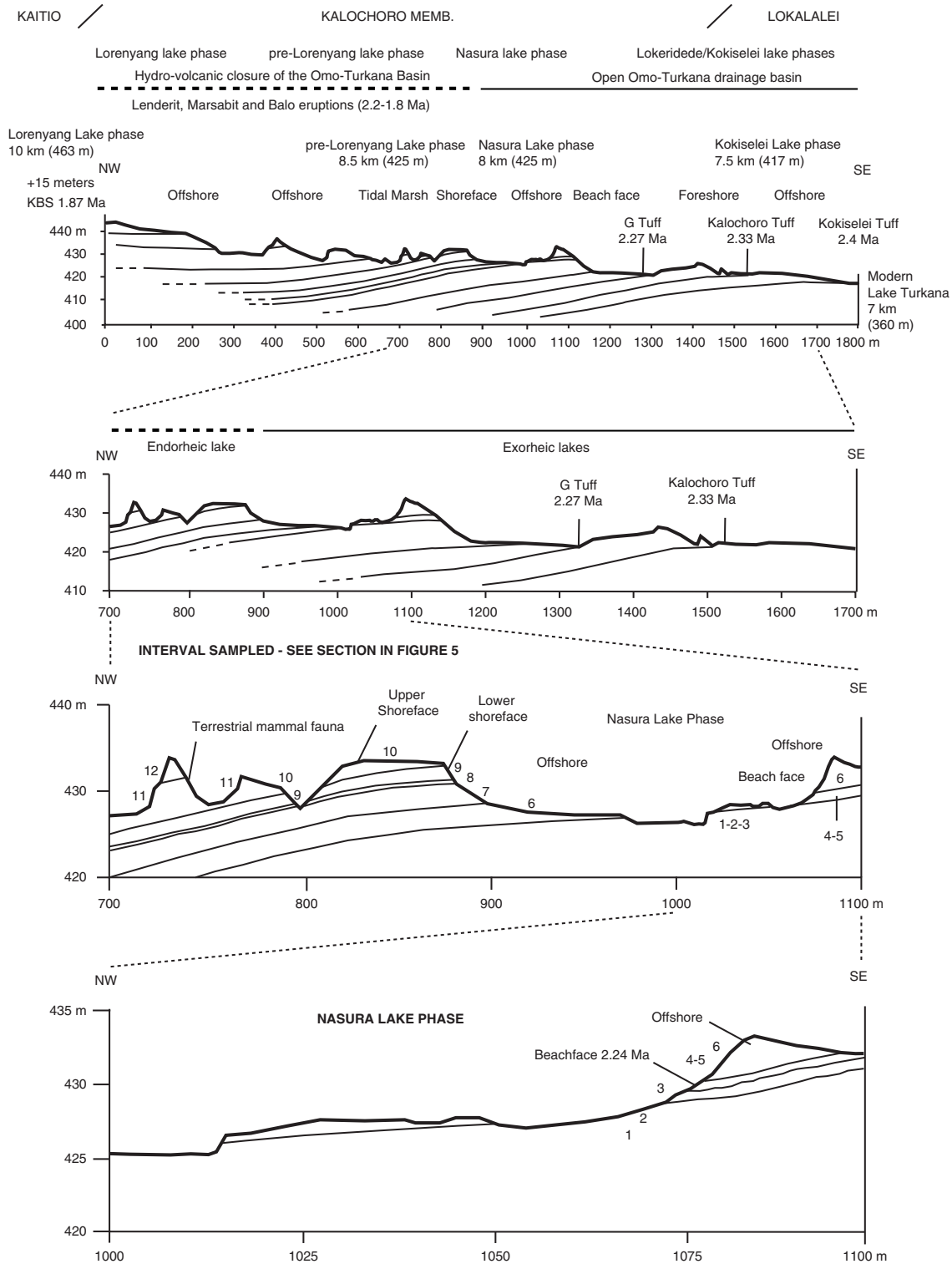

Figure 2. Geologic cross sections with the location of the studied paleolakes and volcanic tuffs. The 2.33 ± 0.02 Ma Kalochoro Tuff delimits the transition between the Lokalalei and Kalochoro Members. The 1.87 ± 0.02 Ma KBS Tuff delimits the Kalochoro and Kaitio boundary. Distances to modern Lake Turkana are reported for each paleolake phase. Numbers denote lithostratigraphic units described in Figure 5.

localities. The volcanic beds that correspond to the GPS coordinates of the identified beds are Kokiselei, Kalochoro, and G (see Table 1 for the coordinates of the tuffs). This confirms interpretations made in the field, based on the geology of the members after Harris et al. (1988). For the KBS Tuff, a bentonite found at the transition between the Kalochoro and Kaitio Members (4°0.375′N, 35°46.553′E; WGS84) corresponds to the KBS bed identified in Lepre et al. (2011).

https://doi.org/10.1017/qua.2018.118 Published online by Cambridge University Press

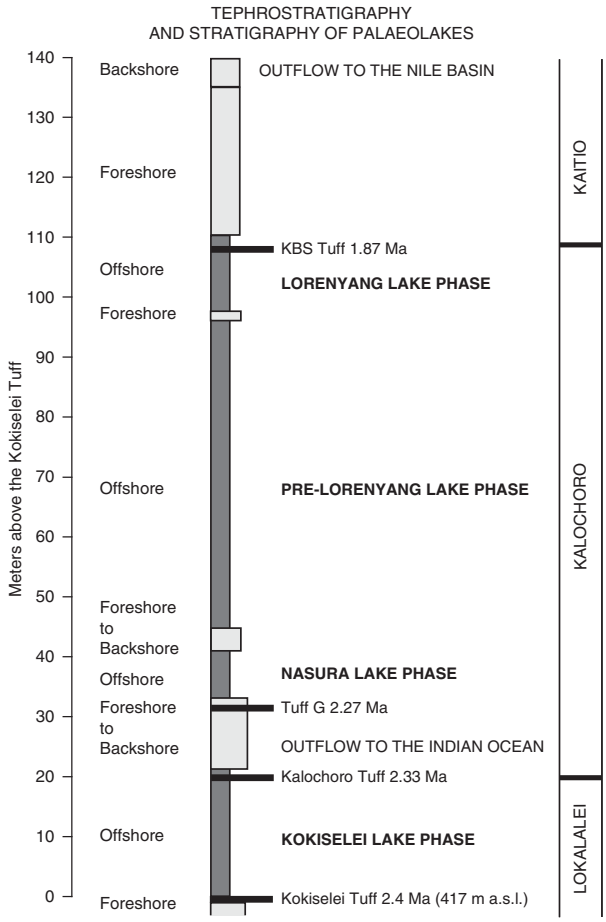

Figure 3. Stratigraphic column of the upper Lokalalei, Kalochoro, and lower Kaitio Members, linking the lacustrine sediments (offshore clays to foreshore sands) with the volcanic tuffs locally identified within these geologic members (see the identified volcanic tuffs presented in the Table 1).

An age model has been calculated using the sedimentation rate estimates between each volcanic bed (Fig. 4). The mean sedimentation rates are 30 cm/ka between the Kokiselei Tuff and Tuff G, and 20 cm/ka between the Tuff G and KBS Tuff. For the interval above the KBS, the sedimentation rate was estimated at 22 cm/ka by Lepre et al. (2011; see also Nutz et al., 2017). The lacustrine cycles are reconstructed along the geologic section from 2.4 to ~1.7 Ma using stratigraphic facies to associate water/depth-controlled sediments to lake-level changes.

Geochemical analyses

The evolution of lake water with depth is also evaluated from the geochemical component of sediment samples collected from 2.26 to 2.19 Ma, just after the onset of volcanic closure of the Omo-Turkana drainage connection to the Indian Ocean (Haileab et al., 2004; Gathogo et al., 2008; Opdyke et al., 2010; Bruhn et al., 2011). Sediment samples have been collected from bottom to top of each type of system (flooding surface, foreshore, offshore, lower and upper shoreface; Fig. 5) that was easily accessible at the Nasura locality (Nasura Lake phase). Superficial sediments were removed before sampling in order to retrieve sediment with as little physical and chemical weathering as possible. Each sample was reduced to powder in an agate ring mill. Major element concentrations (Si, Ti, Mn, Na, P) were analyzed by inductively coupled plasma optical emission spectrometry (Thermo Fischer ICP-OES Icap 6500) at the "Centre de Recherches Pétrographiques and Géochimiques" (CRPG), Nancy, France. Analytical procedures and uncertainties are described in detail in Carignan et al. (2001). Data are reported in Table 2. The precision and accuracy is better than 1% for >10 wt% oxide proportion, within 1–5% for 1–5 wt% oxide proportion and 5–15% for >0.5 wt% oxide proportion. Trace element concentrations (Rb, Sr, Zr, Ca, Ba) were analyzed by inductively coupled plasma mass spectrometry (Thermo Elemental ICP-MS X7) at the CRPG. The precision and accuracy of the analyses were assessed by measuring four rock standards.

Paleohydrologic tracers

The geochemical tracers used to reconstruct paleohydrologic changes in lake sediments are presented in detail in Last and Smol (2006) (see also Yan et al., 2002; Volkova, 1998). In sedimentary successions, strontium (Sr) is normally associated with carbonate minerals, calcite and aragonite in particular (e.g., Cohen, 2003). Strontium can be associated with feldspar and biotite, but at much lower concentrations than in carbonate minerals. In this context, (Zr + Rb)/(Sr + Ca) reflects the balance between clastic (water runoff) and carbonate (stagnant water) components. This relationship expresses foreshore systems in association with (Zr + Rb)/(Sr + Ca) increases. Manganese (Mn) forms a highly insoluble oxide in oxygen-rich waters and migrates up to bottom river and lake sediments (e.g., Cohen, 2003). Manganese is thus a good proxy indicator of vertical transport of oxygen in the water, reflecting decreasing or increasing biological activity. Manganese precipitation could be interpreted as a result of a turnover, when oxygen becomes mixed along the entire water column. The Mn/Ti ratio expresses lake level rise and bottom water oxygenation by wind (offshore systems). Biogenic silica production is evaluated from an elemental ratio: the total amount of silicon oxide (Si)—that is, clastic to biogenic sources—is normalized by the amount of a lithogenic reference element as a proxy for clastic sources only. Titanium oxide (Ti) is chosen, as it is common and relatively abundant. An increase in the Si/Ti ratio is therefore related to high lake productivity in offshore systems (Peinerud et al., 2001). The variations of sodium (Na) in lake sediments can be explained by water runoff and nutrient supply, which is essential for growing biomass in aquatic environments (offshore systems). The excess of sodium in offshore clays is estimated from Na/Ti in comparison with Si/Ti. Zirconium (Zr) is a good proxy indicator of allochthonous siliciclastic inputs (shoreface systems). Zirconium as well as Rubidium (Rb) is common in fluviolacustrine mineral assemblages. Rubidium has its highest concentration in the $< 2\,\mu m$

https://doi.org/10.1017/qua.2018.118 Published online by Cambridge University Press

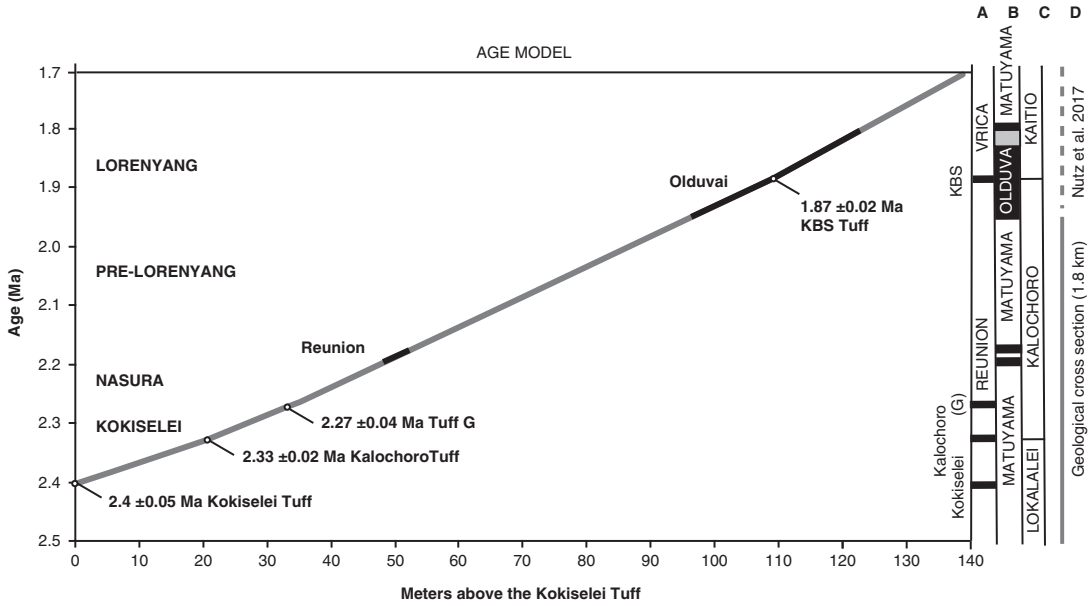

Figure 4. Age models obtained for the 1.8-km-long geologic cross section presented in Figures 2 and 3. The stratigraphic distances are measured in meters above the Kokiselei Tuff with a total station. Ages for the Reunion events are placed according to Quidelleur et al. (2010) and Singer et al. (2014).

fraction (i.e., clays), whereas Zr is linked to silts and heavy mineral enrichment. In the fine-grained lacustrine sediments, Zr/Rb ratio can therefore be used as a grain size proxy, with lower values representing fine-grained material in lower shoreface systems and higher values representing coarse-grained material in upper shoreface systems. Authigenic calcium (Ca) is very sensitive to thermal changes (e.g., Kelts and Talbot, 1990). Calcium carbonate has both allogenic (erosion) and authigenic (photosynthesis) sources. The authigenic production is evaluated from Ca/Rb and Ca/Sr. An increase in the ratio is therefore regarded as indicating increased authigenic carbonate precipitation. This trend is associated with thermal stratification of a water body, low inflows, and/or high evaporation with algae and microbial activities such as cyanobacteria blooms (expansion and proliferation of cyanobacteria toxins in water). In our paleohydrologic context, thermal stratification and evaporation increase refer to endorheic/closed basin conditions, by contrast to exorheic/open basin conditions. Phosphorous (P) is a good proxy indicator of lake water eutrophication (excess of nutrients, algal blooms, and toxic water). Dissolved barium (Ba) with alkalinity in the water column supports the application of Sr/Ba ratios as a proxy for paleoalkalinity and endorheic conditions: barium is an alkaline-earth metal that is found in more than 80 minerals, principally barite ($BaSO_4$; see McGrath et al., 1989).

RESULTS

Age and cyclostratigraphy of Turkana lakes

A total of four lake phases have been dated between 2.4 and ~1.76 Ma (Figs. 2, 3): Kokiselei Lake phase (2.4 to 2.3 Ma), Nasura Lake phase (2.25 to 2.2 Ma), and pre–Lorenyang and Lorenyang Lake phases (2.17 to ~1.76 Ma). Here the "pre–Lorenyang Lake phase" refers to the lake evolution from 2.17 to ~1.95 Ma, whereas "Lorenyang Lake phase" refers to the lake evolution from ~1.95 to ~1.76 Ma only. The Kokiselei Lake phase is exposed within the upper Lokalalei Member; the Nasura Lake phase occurs within the lower Kalochoro Member (Fig. 2). The pre–Lorenyang Lake phase expands within the lower and upper Kalochoro Member, and the Lorenyang Lake phase occupies the upper Kalochoro Member and lower Kaitio Member (Fig. 2). Each of these lake phases is marked by offshore clays interrupted by foreshore sands (Figs. 2, 3).

At the bottom of the stratigraphic record, foreshore sand deposits include the Kokiselei Tuff at 2.4 Ma (Figs. 2, 3). This depositional environment evolves to offshore clays from the Kokiselei Lake phase (2.4 to 2.3 Ma, including the Kalochoro Tuff at 2.33 Ma; Figs. 2, 3). The offshore clays are replaced by foreshore sands at ~2.29 Ma, including the G Tuff at 2.27 Ma (Figs. 2, 3). The foreshore deposits include a flooding surface with pebbles that are overlain by sands with numerous traces of nest-excavating activities of fish (Fig. 5; i.e., trace fossil of *Piscichnus*; see Feibel, 1987). The fish nests are immediately overlain by a beachface system of sandstone and packstone with dense accumulation of freshwater mollusc shells of various species attributable to washover (*Melanoides* sp., *Bellamya* sp., *Cleopatra* sp.; Fig. 5). This is overlain by offshore clays containing some fish bones (Fig. 5) at 2.25 Ma, forming the beginning of the Nasura Lake phase. These offshore deposits are overlaid by lower and upper shoreface silts with ripples at 2.2–2 Ma from the end of the Nasura Lake phase. This depositional environment rapidly changes from

https://doi.org/10.1017/qua.2018.118 Published online by Cambridge University Press

Table 1. Geochemical correlations for tephra sampled at the Nasura locality. All values are in wt%. Analytical methods as reported in Roman et al. (2008) for K07 samples and Haileab (1995) for ETH samples. S, Shungura; WT, West Turkana.

Z	Shard	SiO_2	TiO_2	ZrO_2	Al_2O_3	Fe_2O_3	MnO	MgO	CaO	Ba	Na_2O	K_2O	F	Cl	Total	N	Locality	GPS	Latitude	Longitude
Tuff G																				
WT	K07-7820av	71.82	0.12	na	10.58	2.99	0.08	0.03	0.14	na	5.19	2.29	0.1	0.18	93.53	16	Nasura. CSF07-2.20	07-370	4°0.139'N	35°47.575'E
S	ETH210. M1	72.52	0.17	0.16	10.62	2.76	0.1	0.03	0.15	0.01	2.39	2.87	0.1	0.12	92	17	Shungura			
Kalochoro Tuff (= Tuff F)																				
WT	K07-7797av	71.09	0.18	na	9.59	4.68	0.16	0.02	0.18	na	3.47	1.7	0.11	0.16	91.35	9	Nasura. CSF07-2.11	07-334	4°0.126'N	35°47.706'E
S	ET-51	69.55	0.23	0.19	9.62	4.6	0.19	0.01	0.18	0.01	1.4	1.91	0.01	0.14	88		Shungura			
Kokiselei Tuff (= Tuff E)																				
WT	K07-7796/1AV	74.01	0.42	na	8.65	6.09	0.25	0.11	0.18	na	1.24	1.78	0.02	0.22	92.9	8	Nasura. CSF07-2.2	07-333	4°0.185'N	35°47.951'E
S	ETH86-183. M3	72.32	0.35	na	8.74	6	0.27	0.11	0.19	na	0.86	2.01	na	0.16	91.01	13	Shungura			

foreshore to backshore deposits enriched in terrestrial mammal fossils (such as hippopotamus and elephant; see also the description of the same level in Harris et al. [1988]) at ~2.18 Ma. Immediately above this surface, the offshore clays from the pre–Lorenyang Lake phase (2.17 to ~1.95 Ma) occur ~25 m above the Kalochoro Tuff and ~45 m above the Kokiselei Tuff; Fig. 3). From 2.17 to ~1.95 Ma, the depositional environments are characterized by low-energy dynamics (offshore muds to shoreface silts; Figs. 2, 5). The same depositional environment continues until 1.87 Ma (KBS Tuff) through the Lorenyang Lake phase. The Lorenyang Lake phase is then characterized by higher-energy dynamics and by an accretion of successive foreshore to backshore deposits from 1.87 to ~1.76 Ma (see section in Nutz et al., 2017). This system is overlaid by oncolite-rich silts to fine sands from ~1.76 to 1.72 Ma (including the Olduvai/Matuyama paleomagnetic transition; see Lepre et al., 2011). If we consider that the sediments were affected by subsidence since the early Pleistocene, these lake sediments still occur at the level of the outflow sill to the west and the Nile basin (~460 m). The total thickness of the lake sediments above the Kokiselei Tuff suggests that the level of the lake was +100 m above Kokiselei Lake level during the Lorenyang Lake phase (see Fig. 3).

Our data show that from 2.4 to 1.87 Ma, offshore clays occur synchronously with 100 ka insolation maxima and foreshore silts to sands with 100 ka insolation minima (Fig. 6). An asynchronous lake phase is, however, found at 2.17 to ~1.95 Ma (Fig. 6) during a 400 ka insolation minimum. During this asynchronous lake phase, the level of the lake had risen up to +50 m (Fig. 3).

Evolution of lake water

Prior to 2.17 Ma, the paleohydrologic evidence indicates that the lake waters were still well mixed at the beginning of the lake transgression: the (Zr + Rb)/(Sr + Ca) ratio suggests an increase of water runoff from 2.26 to 2.24 Ma (Fig. 7). The Mn/Ti ratio suggests also that the lake waters were still well oxygenated at 2.24–2.23 Ma, during the insolation maximum (Fig. 6). As a consequence, lake productivity probably increased, as water runoff and photosynthesis increased at the same time (Si/Ti, Na/Ti increases). The comparison between Si/Ti and Na/Ti suggests that nutrients increased from 2.24 to 2.22 Ma, still during the insolation maximum (Fig. 6), but lake productivity collapsed after 2.22 Ma, which corresponds with the transition between offshore clays to shoreface silts (Figs. 5, 7). The top of the offshore mud package is overlain by a lower shoreface system composed of silts with typical wind-blown ripples (Fig. 5). The period at 2.22–2.21 Ma is associated with the progradation of an upper shoreface system containing some distinct beds enriched in fish bones (freshwater catfish group; Fig. 5). The upper shoreface silts contain small fish debris beds along bedding planes and gypsum coatings. The sediments show an enrichment of silts versus clay from Zr/Rb ratios (Fig. 7).

https://doi.org/10.1017/qua.2018.118 Published online by Cambridge University Press

Table 2. Geochemical results obtained from the composition of bulk sediments of the Nasura Lake phase (see also Fig. 7). See text for explanations.

Meters above Kokiselei Tuff (m)	Lithology	Age Ma	SiO_2 %	Al_2O_3 %	Fe_2O_3 %	Na_2O %	CaO %	K_2O %	MgO %	TiO_2 %	P_2O_5 %	MnO %	Ba ppm	Sr ppm	Zr ppm	Rb ppm
46.0	Brownish gray clay (swamp)	2.19	52.28	13.61	9.11	2.20	2.78	2.269	2.64	1.58	0.4	0.11	394.9	250	257	53
44.5	Brownish gray silts (upper shoreface)	2.195	53.66	13.85	9.17	2.86	3.22	2.149	2.18	2.01	0.54	0.15	428	340	362	57
44.0	Brownish gray silts (upper shoreface)	2.2	54.22	14.20	9.58	2.92	2.72	1.95	2.36	2.07	0.38	0.12	419.4	359	369	55
43.0	Brownish gray silts (upper shoreface)	2.205	54.34	14.77	9.58	3.30	2.86	1.88	2.23	2.32	0.35	0.13	458.8	396	369	51
42.0	Brownish gray silts (upper shoreface)	2.21	55.82	14.31	9.30	3.34	3.86	1.86	2.36	2.06	0.25	0.17	429.3	427	348	51
41.0	Brownish gray silts (upper shoreface)	2.215	54.00	14.80	10.02	3.48	4.00	1.84	2.34	2.42	0.27	0.15	492	450	301	47
40.5	Brownish gray silts (fish bones in lower shoreface)	2.22	54.25	15.16	9.12	3.47	3.84	1.82	2.48	2.00	0.27	0.17	440.6	463	355	48
40.0	Brownish gray silts (lower shoreface)	2.225	56.85	15.22	7.83	3.72	2.70	2.10	1.80	1.53	0.21	0.11	491.3	413	335	54
39.0	Brownish clay (offshore laminated)	2.228	57.96	15.44	6.73	3.83	2.41	2.29	1.4	1.55	0.19	0.10	478.2	382	381	58
38.5	Brownish clay (offshore)	2.23	57.35	15.68	6.84	3.79	2.64	2.27	1.53	1.62	0.22	0.15	496.4	382	379	54
37.5	Brownish clay (offshore)	2.235	51.88	14.30	9.50	2.72	1.98	1.77	1.9	1.94	0.23	0.07	333.2	286	382	60
36.5	Brownish clay (offshore)	2.24	54.66	15.62	9.21	3.62	2.53	2.08	1.45	2.08	0.24	0.13	472	388	330	55
36.0	Sandstone (*Melanoides* in beachface)	2.245	51.06	14.28	10.88	2.37	1.98	1.50	2.14	2.01	0.25	0.08	296	279	383	58
34.0	Light brownish sandy clay (*Piscichnus*)	2.25	51.87	14.56	12.38	2.80	1.72	1.86	1.48	2.15	0.22	0.11	363.1	245	401	56
33.5	Brownish gray clayey silt (flooding surface)	2.26	58.48	15.09	8.93	3.43	2.26	2.11	1.46	1.50	0.2	0.08	575.7	402	211	51

The water level progressively diminished after 2.21 Ma, as seen from Ca/Rb ratio decreases and Ca/Sr ratio increases (see Fig. 7), illustrating the evolution of the Ca source. From 2.22 to 2.21 Ma, the source of Ca was lake carbonate precipitation in the lower and upper shoreface (Ca/Rb and Ca/Sr increase). After 2.21 Ma, the Ca source changes from lake (upper shoreface) to more terrestrial sources (abiogenic: Ca/Rb decrease and Ca/Sr increase). The precipitated lake carbonate estimated from Ca/Rb ratio suggests that photosynthesis increased from 2.22 to 2.21 Ma in the lower and upper shoreface, and then decreased after 2.21 Ma during lake regression (Fig. 7). Carbonate was less soluble, and thus biogenic carbonate did not precipitate after 2.21 Ma (Fig. 7). Alkalinity increased from 2.22 to 2.21 Ma as suggested from Sr/Ba ratios (Fig. 8), if we consider that the distribution of dissolved barium in the lake water changes with alkalinity. This evolution illustrates the end of the Nasura Lake phase at ~2.2 Ma, which occurred during an insolation minimum centered at 2.17 Ma. After this chronostratigraphic level, P/Ti ratio increased as the lake system was rapidly replaced by a short-lived swamp with mammalian bones at ~2.18 Ma (Fig. 7). Lake waters were probably toxic at that time because of nutrient increase and algal blooms (probably toxic cyanobacteria). The horizon enriched by terrestrial fossils is rapidly replaced by offshore muds at 2.17 Ma (onset of pre–Lorenyang Lake phase).

DISCUSSION

Monsoonal and astronomical forcing on Turkana lakes

Although located in the arid Turkana depression, Lake Turkana is supported by the monsoon rains in Omo River highlands (Joordens et al., 2011). The contribution of the East African monsoon is caused by the zonal advection of Indian Ocean–derived moisture to the Ethiopian highlands (Camberlin, 1997). The East African monsoon rains reflect the northward movement of the Intertropical Convergence Zone over East Africa (see, e.g., Nicholson, 1996, 2009). The "long rains" reach a northward limit in summer coeval with a maximum discharge from the Omo River (Bloszies and Forman, 2015). On the astronomical time scale, changes in eccentricity, insolation, and precession cycles control the strength of vapor transport and monsoons (Merlis et al., 2013). In the tropical highlands/forests, the summer monsoonal moisture increases during eccentricity/insolation maxima (Rossignol-Strick, 1983). In addition, with the initiation of Northern Hemisphere glaciation paced by 100 ka eccentricity/insolation cycles (Lisiecki, 2010; Abe-Ouchi et al., 2013), monsoonal climate was controlled by the development of cold glacial North Atlantic sea surface temperature (see deMenocal, 1995). Thus, the East African

https://doi.org/10.1017/qua.2018.118 Published online by Cambridge University Press

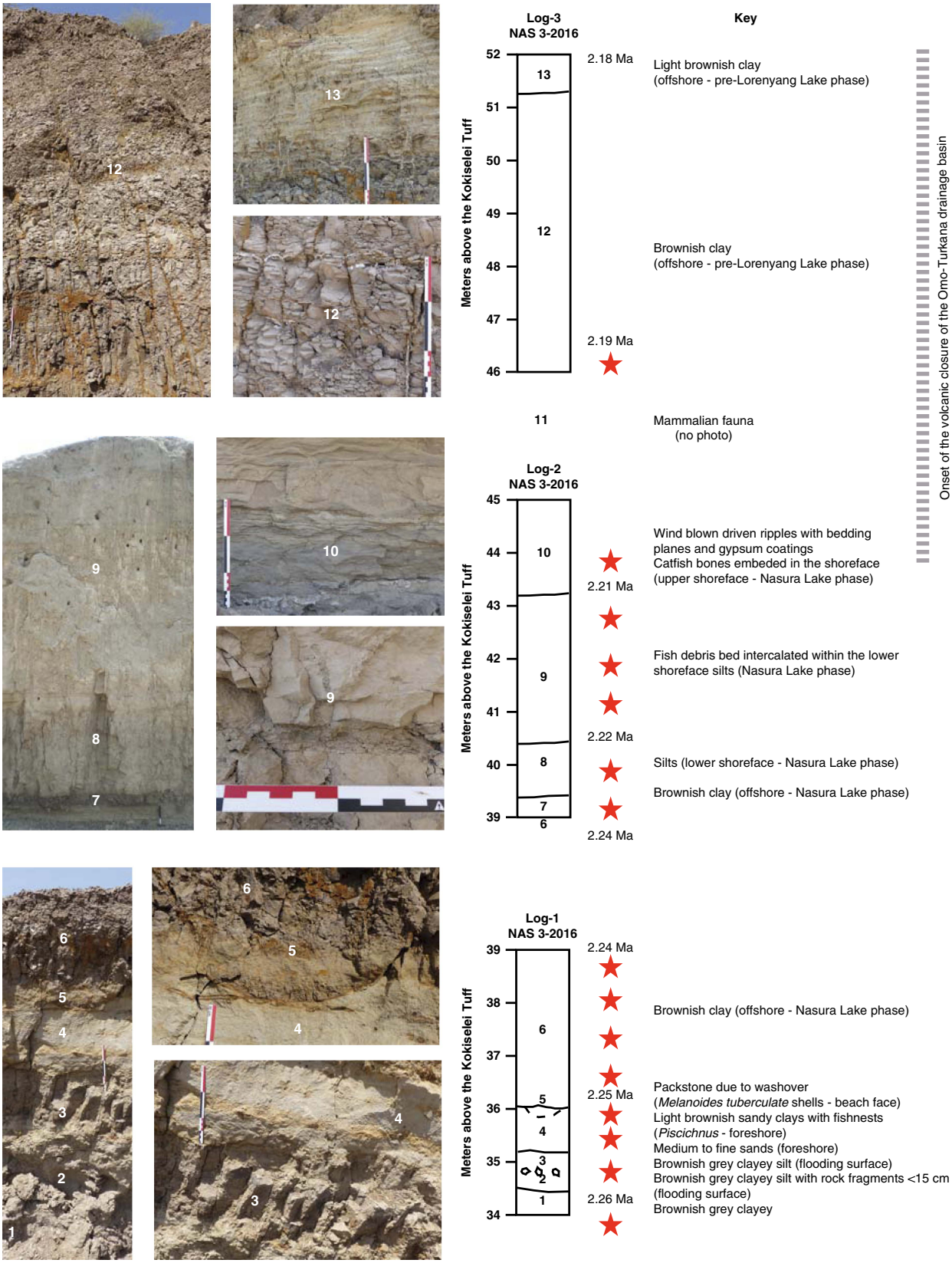

Figure 5. Lithology and stratigraphy of the Nasura Lake phase (Nasura locality). The red stars represent the analyzed geochemical samples. See Figure 2 for the location of the examined outcrops. (For interpretation of the references to color in this figure legend, the reader is referred to the web version of this article.)

https://doi.org/10.1017/qua.2018.118 Published online by Cambridge University Press

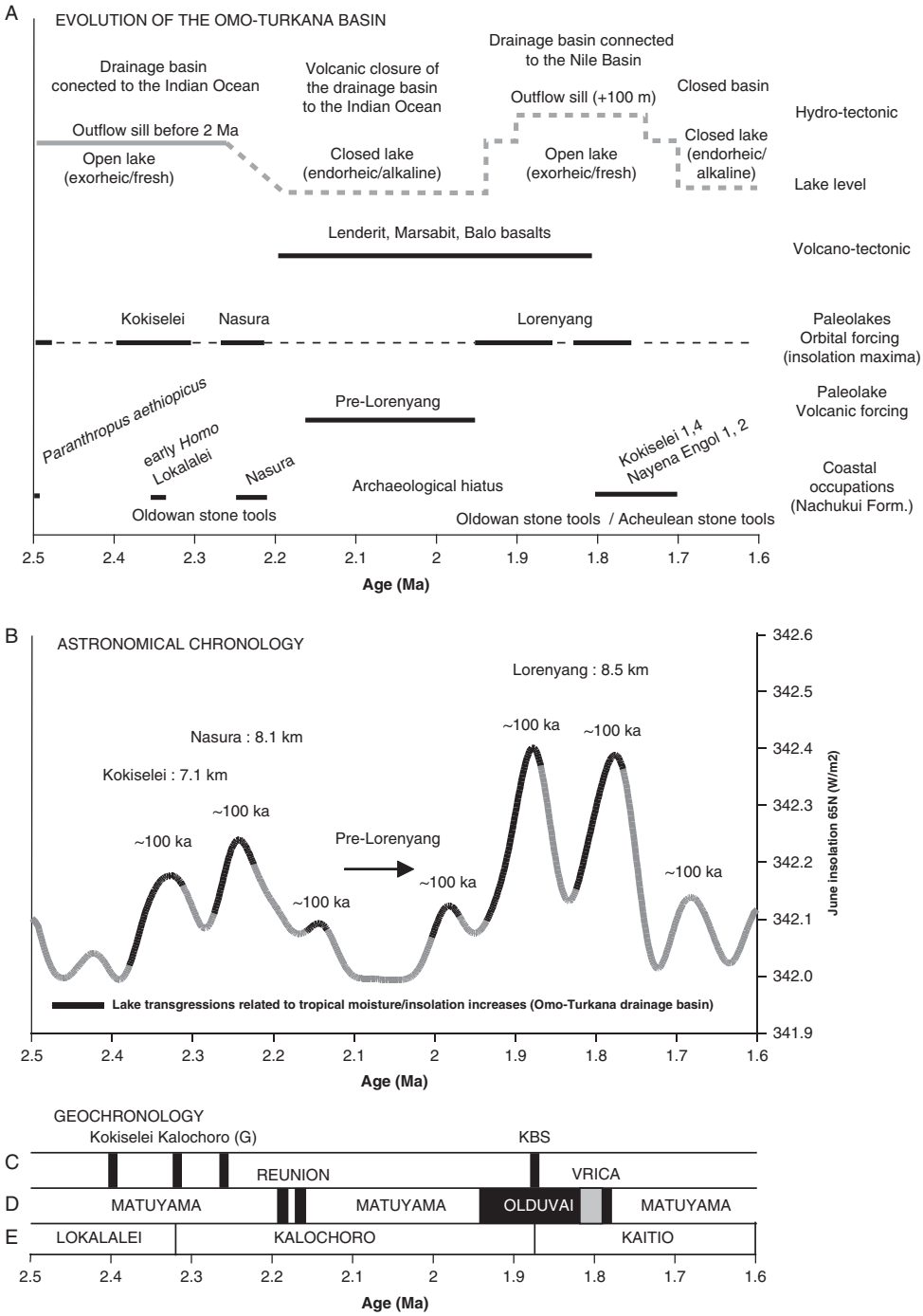

Figure 6. Comparison of different information from 2.5 to 1.6 Ma. (A) Volcano-tectonic evolution of the Omo-Turkana drainage basin (after Bruhn et al., 2011) and limnological evolution of paleolakes; astronomical and tectonic forcing on the lake phases; coastal occupations (after Walker et al., 1986; Roche et al., 2003; Prat et al., 2005; Lepre et al., 2011) in relation to the insolation cycle. (B) Evolution of the paleolakes in relation to the 100 and 400 ka components of insolation cycle (after Laskar et al., 2004). We have taken June insolation at 65°N because of the influence of the Northern Hemisphere glaciation on African climate and thermohaline circulation between 3 and 2 Ma (see Gupta and Thomas, 2003; see also Raymo et al., 1992). (C) Argon-argon dated tuffs of the Nachukui Formation (after McDougall et al., 2012). (D) Magnetostratigraphy of the Nachukui Formation; ages for the Reunion events are placed according to Quidelleur et al. (2010) and Singer et al. (2014). (E) Geologic members of the Nachukui Formation (after Harris et al., 1988).

monsoons increased in duration and strength during the early Pleistocene (Gupta et al., 2001; Gupta and Thomas, 2003; see also Raymo et al. [1992] for the influence of thermohaline circulation between 3 and 2 Ma).

Influence of insolation on lake level changes

As suggested by our data, the insolation cycle plays a role in lake level changes and coastal geomorphology in the Turkana

https://doi.org/10.1017/qua.2018.118 Published online by Cambridge University Press

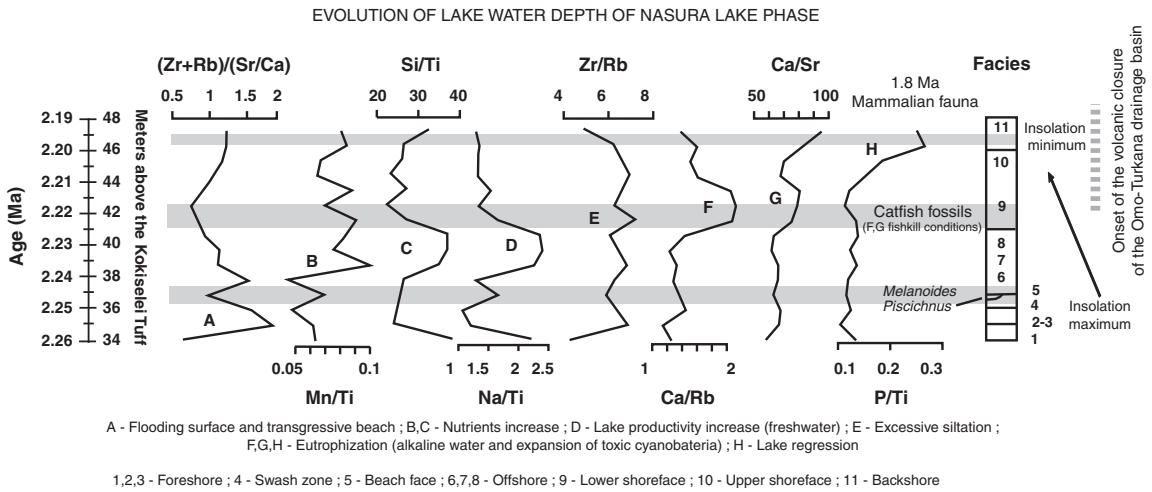

Figure 7. Evolution of lake depth reconstructed from geochemical tracers and evolution of the depositional environments from 2.26 to 2.19 Ma, including paleolimnological/thermal evolution of the Nasura Lake phase, concomitant to volcanic closure of the Omo-Turkana drainage basin.

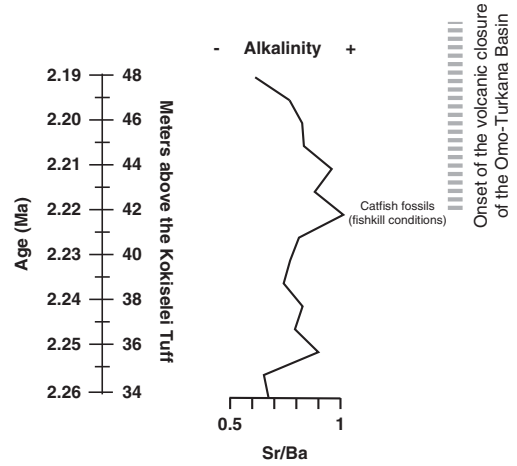

Figure 8. Evolution of the Nasura Lake phase during tectonic closure of the Turkana drainage connection to the Indian Ocean. Alkalinity and water turbulence are estimated from Sr/Ba ratio.

basin (see also Nutz et al. [2017] for similar observation in the Turkana basin, Kingston et al. [2007] in the Baringo basin, and Ashley [2007] in the Olduvai basin). Turkana paleolake levels should increase during higher monsoonal inflows from the Omo River every 100 ka insolation/eccentricity maximum (Figs. 6, 9). In our record, Turkana paleolake levels indeed appear to rise in response to the 100 and 400 ka components of the insolation/eccentricity maxima cycle (Figs. 6, 9). At the bottom of our record, the Kokiselei and Nasura Lake phases can be explained by the increase in monsoonal moisture available in the tropical Ethiopian highlands during the 100 and 400 ka component of the cycle centered at 2.24 Ma (Figs. 6, 9). However, from 2.17 to ~1.95 Ma, the pre–Lorenyang Lake phase expands during a 400 ka insolation minimum centered at 2.0 Ma (Figs. 6, 9), and the depositional environments evolve rapidly toward offshore system (+50 m of lacustrine muds; Fig. 3) . This main paleolake phase is not in good synchronicity with insolation/eccentricity forcing and hydroclimatic context, implying that a different factor was involved – namely, volcanism.

Influence of volcanism

Volcanism has reorganized the course of the Omo River from the Ethiopian highlands through Turkana to either the Mediterranean Sea or the Indian Ocean, greatly modulating paleolake responses to astronomical forcing factors during the early Pleistocene (Watkins, 1986; Haileab et al., 2004; Gathogo et al., 2008; Opdyke et al., 2010; Bruhn et al., 2011). From 2.2 to 1.8 Ma, different channel outlets were cut off by the eruptions of the Lenderit (2.2–2 Ma), Marsabit (2.0–1.8 Ma), and Balo (1.8 Ma) lava flows at the south end of the Turkana rift segment (Bruhn et al., 2011). These volcanic events progressively caused the closure of the Omo-Turkana outflow sill to the Indian Ocean and may therefore be responsible for the pre–Lorenyang Lake phase (Figs. 6, 9). During these eruptions, Paleolake Turkana probably alternated from endorheic/alkaline to exorheic/freshwater because several river outflows were successively connected and disconnected with the Indian Ocean by lavas. Exorheic conditions returned during the insolation/eccentricity maxima at 1.9 to 1.8 Ma, as the lake rose up to +100 m above the closed outflow to the east and a new outflow sill temporary opened toward the west and the Mediterranean Sea. Stable isotope records ($\delta^{18}O$ and $\delta^{13}C$) of fossil bivalve shells confirm that Lake Turkana was temporarily exorheic/fresh around 1.9 Ma (Lorenyang and G Tuff level; Vonhof et al., 2013). After 1.7 Ma, this outflow sill was closed by the lake level fall, and the outflow sill to the Indian Ocean was blocked by Lenderit, Marsabit, and Balo basalts. Thus, Lake Turkana became more permanently endorheic since these volcanic events that transformed the evolution of the drainage basin during the early Pleistocene. Our reconstruction echoes the interpretations from Bruhn et al. (2011) and Lepre (2014),

https://doi.org/10.1017/qua.2018.118 Published online by Cambridge University Press

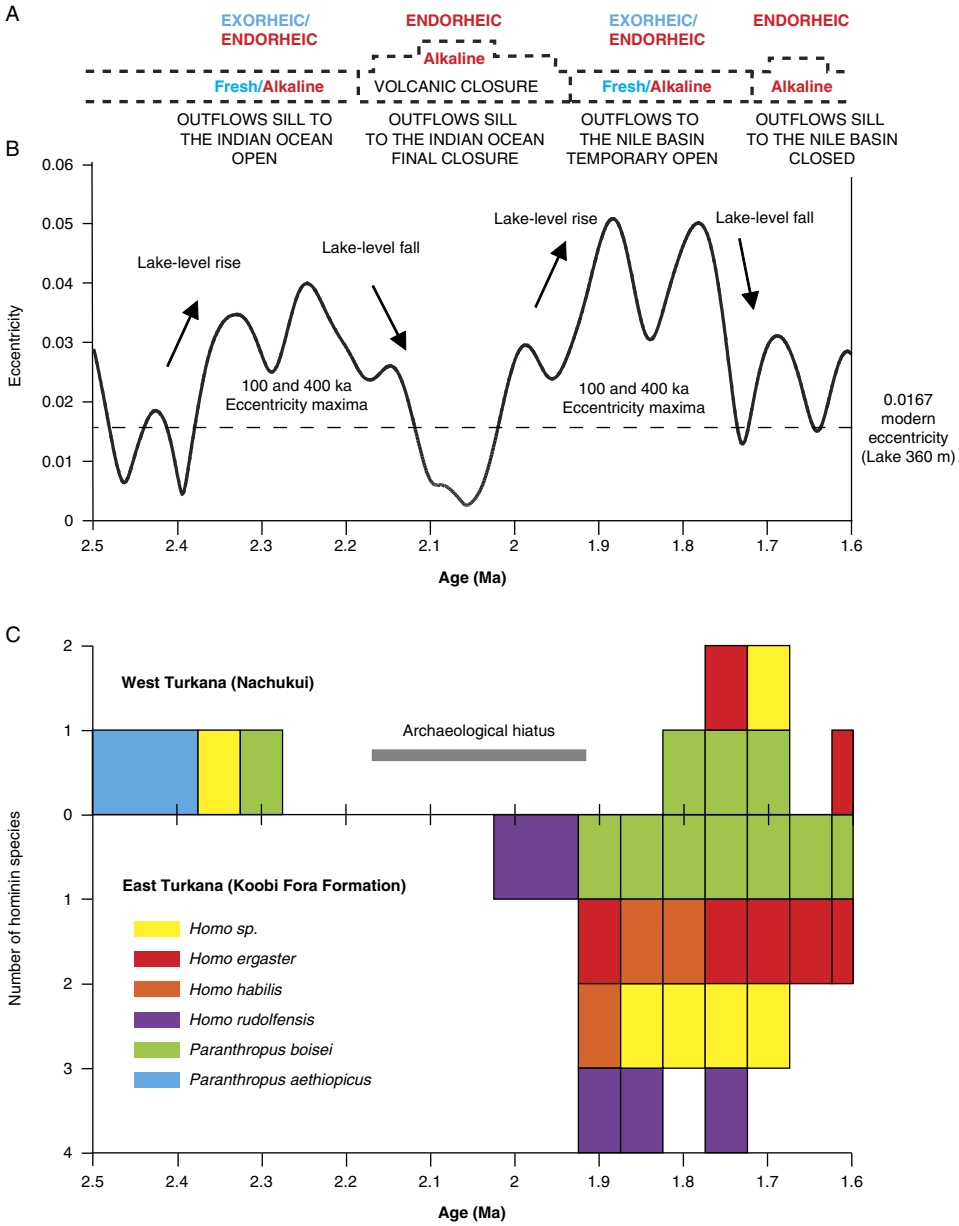

Figure 9. (color online) Comparison of the hydrovolcanic-tectonic evolution of the Turkana basin, the eccentricity cycles, and hominin occurrences between 2.5 and 1.6 Ma. (A) Evolution of Lake Turkana water and limnology. (B) Earth's eccentricity cycles (after Laskar et al., 2004). (C) Number of hominin species found in the Nachukui Formation and in the Koobi Fora Formation from 2.5 to 1.6 Ma (specimens allocated to hominin indet. were not included).

which suggested a nonclimatic origin for the onset of the pre–Lorenyang lake phase in the Turkana basin.

Lake water evolution following volcanic closure of the Omo River outflows to the Indian Ocean

In central Kenya, Bergner et al. (2009) have suggested that rift lakes evolve toward freshwater ecosystems during humid–high lake phases and revert back to alkaline conditions during arid–low lake phases. In Turkana, volcanism probably played also a role in lake level evolution and paleoalkalinity. In our paleochemical record (Figs. 7, 8), the Sr/Ba ratio suggests that paleolakes evolved toward more alkaline conditions at the end of the Nasura Lake phase, which could be attributable to the onset of hydrovolcanic closure of the Omo-Turkana basin. Our data suggest that Paleolake Turkana had alkalinity increase around 2.22–2.21 Ma, where more dense fish debris beds are found in the upper shoreface. Two main mechanisms can be proposed for the occurrence of these dense fish debris beds. Methane-producing bacteria in lake-floor sediments may generate excess methane gas in the lake waters if the production rate is higher than the diffusion rate in the uppermost layers (Caliro et al., 2008). This interpretation would be consistent with

https://doi.org/10.1017/qua.2018.118 Published online by Cambridge University Press

temperature increase, high microbial photosynthesis activity during the day, and abrupt oxygen depletion during the night. The fish debris beds could therefore be interpreted as mass fish die-off events explained by critical limnological conditions for the fish: a negative oxygen balance between day and night or alkalinity increase (*Tilapia* can survive with alkalinity of 40 meq/L, but less adaptable fish are absent). According to Cerling (1979), concentration of consistently small-size fish remains may indicate high salinities and alkalinities that exceeded 40 meq/L. Thus, alkalinity increase would explain the accumulation of fish debris within wind-driven beds formed within the shoreface. Another hypothesis is that the fish debris beds were caused by an overturn of the water column and hydrogen sulfide saturation during a major underwater disturbance (i.e., an earthquake or volcanic eruption) as has been observed in modern lakes (Caliro et al., 2008).

The paleochemical range of the ostracods (Cohen, 1981) also shows that alkalinity increased during the closure of the drainage connection to the Indian Ocean (see also Abell [1982] for alkalinity fluctuations during the same interval). Comparatively, freshwater malacofauna and paleochemistry of Lake Turkana suggest that paleolakes were fresh during the late Pliocene with an alkalinity range from 2 to 8 meq/L (Cerling, 1979; Bocxlaer et al., 2008; Bocxlaer, 2011). According to Cerling (1979), freshwater molluscs could survive in East African waters with an alkalinity range of about 0.5 to 15 meq/L. In Lake Turkana, freshwater mollusc extinction occurs at an alkalinity of ~16 meq/L (Abell, 1982). In East Turkana, freshwater molluscan assemblages (Williamson, 1982; Bocxlaer et al., 2008) gradually impoverish upward in the Okote Member, which is equivalent to the Natoo Member (1.6–1.3 Ma) in West Turkana. Fossils of endemic freshwater stingrays (*Dasyatidae)* found within the Turkana basin suggest that freshwater conditions persisted until ~1.6 Ma (see Feibel, 1994).

Implications for hominin coastal occupations

Most of the archaeological sites and terrestrial fossils (including hominins) are trapped within lake margin deposits formed during 100 ka insolation/eccentricity maxima and fresh–high lake phases (Figs. 6, 9). For example, the 2.34 Ma archaeological complex of Lokalalei (Roche et al., 1999) is located within the lower Kalochoro Member, during a 100 ka cycle of insolation maximum centered at 2.33 Ma. Most of the Lokalalei sites are found above the 2.34 Ma Ekalalei Tuff (Kibunjia et al., 1992; Kibunjia, 1994; Roche et al., 1999; Prat et al., 2005; Tiercelin et al., 2010). The archaeological sites of Kokiselei 4 (1.76 Ma; Lepre et al., 2011), Kokiselei 1 (1.79–1.69 Ma; Prat et al., 2003; Roche et al., 2003), Naiyena Engol 1 (1.75 Ma; Prat et al., 2003; Roche et al., 2003) and 2 (1.8–1.7 Ma; Roche et al., 2018) occur during fresh–high lake phases related to the insolation maximum centered at 1.77 Ma and transition toward the beginning of an insolation minimum.

Before ~2.17 Ma, freshwater lakes driven by insolation maxima were not necessarily high in elevation, because the outflow sill to the Indian Ocean was ~100 m lower than the outflow sill to the Nile basin. Although not necessarily high, lakes that outflowed to the Indian Ocean were exorheic and fresh. After ~2.17 Ma, freshwater lakes driven by insolation maxima had to rose up to +100 m above the closed outflow sill to the Indian Ocean, so they potentially reached the outflow sill to the Nile basin (Figs. 2, 3, 6, 9). In this context, archaeological sites occur during exorheic/freshwater lake phases driven by insolation maxima. Comparatively, periods of insolation minima are associated with hydrologic conditions that were more endorheic/alkaline with "archaeologically sterile" sediments (Fig 6).

In the Nachukui Formation, researchers noted the presence of an archaeological hiatus initially evaluated between 2.3 and 1.8 Ma (Roche et al., 2003). The hiatus is now reduced to the period 2.17–1.8 Ma thanks to the discovery of new archaeological sites by the WTAP (Harmand et al., manuscript in preparation). This archaeological hiatus coincides with hydrovolcanic closure of the basin and the development of the endorheic pre–Lorenyang Lake phase (Figs. 6, 9). During the ~2.2–1.95 Ma period of insolation minimum (Fig. 6), the lake margins may not have contained as many suitable onshore environments as during insolation maxima. From 2.17 to ~1.95 Ma, Lake Turkana expanded but had no outflows and was endorheic/alkaline and not exorheic/fresh. The hydrologic conditions were probably not as suitable for hominin occupations as when the lake was exorheic/fresh. This is suggested by the temporal distribution of coastal archaeological sites and hominin occupations around the lake (Figs. 6, 9). No archaeological sites are found through the pre–Loreyang Lake phase (Fig. 6). Hominin occupations are found again from ~1.8 to 1.7 Ma, during insolation/eccentricity maxima, as freshwater/exorheic conditions were temporary restored by lake level rise up to the outflow sill to the west and the Mediterranean Sea.

CONCLUSIONS

Today, the Turkana basin is home to the largest endorheic alkaline-saline lake in an arid environment on Earth. This terminal lake is supplied by the Omo River, and its water level (360 m asl) is in equilibrium with evaporation output. The particularity of Lake Turkana is that over its long-term evolution, the lake alternated from exorheic to endorheic conditions because of volcanic and astronomical forcings, with strong implications for lake water chemistry. Before the early Pleistocene, Lake Turkana outflowed to the east and the Indian Ocean and was exhoreic/open/fresh. Following volcanic closure of the outflow sill to the east in the early Pleistocene (Lenderit, Marsabit, and Balo eruptions from 2.2 to 1.8 Ma), the lake became endorheic/closed/alkaline during periods of insolation/eccentricity minima (low lake levels), like present-day conditions. However, during periods of insolation/eccentricity maxima (high lake levels), the lake became potentially exorheic/fresh when the overflow sill to the west and the Mediterranean Sea was reached (+100 m

https://doi.org/10.1017/qua.2018.118 Published online by Cambridge University Press

above the closed outflow sill to the Indian Ocean). Thus, lake levels changed following the reorganization of the drainage basin in the early Pleistocene, and this should not be interpreted in terms of extreme climate change.

Our study shows that from 2.4 to 2.17 Ma, hominin coastal occupations occur within the lake margin deposits related to insolation/eccentricity maxima and exorheic/freshwater conditions. An archaeological hiatus occurs during insolation/eccentricity minimum from 2.17 to 1.9 Ma, which is concomitant to endorheic/alkaline conditions caused by volcanic closure of the Omo-Turkana drainage basin. Hominin occupations are found again during insolation/eccentricity maximum from 1.8 to 1.7 Ma, as freshwater/exorheic conditions were temporary restored by lake level rise up to the outflow sill to the Mediterranean Sea. In the Turkana basin, the role of volcanism appears to have modulated the role of astronomical forcing on lake level changes. The reorganization of the Omo-Turkana drainage basin during the early Pleistocene seems to have had broad implications for the occupation of the basin by hominins, although no extreme humid-arid climate shifts are involved as previously thought.

ACKNOWLEDGMENTS

This research is based on successive fieldwork with the Mission Préhistorique au Kenya–West Turkana Archaeological Project (MPK-WTAP) in the Turkana basin between 2010 and 2016. We thank the Office of the President of Kenya; the Ministry of Education, Science and Technology of the Republic of Kenya; the National Council for Science and Technology (NCST/RCD/12B/012/25); and the National Museums of Kenya for permission to conduct research in the field. This research was funded by the Agence Nationale de la Recherche (ANR-12-CULT-0006), by the Ministère des Affaires Etrangères (Direction générale de la mondialisation, du développement et des partenariats, N°681/DGM/ATT/RECH, N°986/DGM/DPR/PRG), by the LSB Leakey Foundation, by OASIC/AAP2017-UMI-CNRS-France (Project MobHom), and by S. Para (NTM INDIGO-France). We are particularly grateful to H. Roche who has encouraged this research since the beginning. We thank S. Jeremie, K. Salas Rossenbach, S. Nourissat, and D. Pelletier for their support at INRAP. We also thank F. Brown, M. Schuster, A. Nutz, and C. Lepre for interactive discussions in the field. We thank N. Taylor, S. Clement, M. Brenet, S. Lokorodi, and the 2010–2016 MPK-WTAP team members for assistance in Turkana. We thank D. Booth, T. Faith, and the anonymous reviewers for their constructive comments, which helped to improve the manuscript. This work is dedicated to F. Brown (1943–2017) and Jean-Jacques Tiercelin (1949–2017).

REFERENCES

Abell, P.I., 1982. Palaeoclimates at Lake Turkana, Kenya, from oxygen isotope ratios of gastropod shells. *Nature* 297, 321–323.

Abe-Ouchi, A., Saito, F., Kawamura, K., Raymo, M.E., Okuno, J.I., Takahashi, K., Blatter, H., 2013. Insolation-driven 100,000-year glacial cycles and hysteresis of ice-sheet volume. *Nature* 500, 190–193.

Ashley, G.M., 2007. Orbital rhythms, monsoons, and playa lake response, Olduvai Basin, equatorial East Africa (ca. 1.85–1.74 Ma). *Geology* 35, 1091–1094.

Behrensmeyer, A.K., 2006. Climate change and human evolution. *Science* 311, 476–478.

Bergner, A.G., Strecker, M.R., Trauth, M.H., Deino, A., Gasse, F., Blisniuk, P., Duehnforth, M., 2009. Tectonic and climatic control on evolution of rift lakes in the Central Kenya Rift, East Africa. *Quaternary Science Reviews* 28, 2804–2816.

Bloszies, C., Forman, S.L., 2015. Potential relation between equatorial sea surface temperatures and historic water level variability for Lake Turkana, Kenya. *Journal of Hydrology* 520, 489–501.

Bocxlaer, B., 2011. Palaeobiology and evolution of the late Cenozoic freshwater molluscs of the Turkana Basin: Unionidae Rafinesque, 1820, partim *Coelatura* (Bivalvia: Unionoidea). *Journal of Systematic Palaeontology* 9, 523–550.

Bocxlaer, B., Damme, D.V., Feibel, C.S., 2008. Gradual versus punctuated equilibrium evolution in the Turkana Basin molluscs: evolutionary events or biological invasions? *Evolution* 62, 511–520.

Bonnefille, R., 2010. Cenozoic vegetation, climate changes and hominid evolution in tropical Africa. *Global and Planetary Change* 72, 390–411.

Brown, B., Brown, F.H., Walker, A., 2001. New hominids from the Lake Turkana basin, Kenya. *Journal of Human Evolution* 41, 29–44.

Brown, F., Harris, J., Leakey, R., Walker, A., 1985. Early *Homo erectus* skeleton from west Lake Turkana, Kenya. *Nature* 316, 788–792.

Brown, F.H., Feibel, C.S., 1988. "Robust" hominids and Plio-Pleistocene palaeogeography of the Turkana Basin, Kenya and Ethiopia. In: Grine, F. (Ed.), *Evolutionary History of the "Robust" Australopithecines*. Aldine de Gruyter, New York, pp. 325–341.

Brown, F.H., McDougall, I., 2011. Geochronology of the Turkana depression of northern Kenya and southern Ethiopia. *Evolutionary Anthropology* 20, 217–227.

Brown, F.H., Sarna-Wojcicki, A.M., Meyer, C.E., Haileab, B., 1992. Correlation of Pliocene and Pleistocene tephra layers between the Turkana Basin of East Africa and the Gulf of Aden. *Quaternary International* 13, 55–67.

Bruhn, R.L., Brown, F.H., Gathogo, P.N., Haileab, B., 2011. Pliocene volcano-tectonics and palaeogeography of the Turkana Basin, Kenya and Ethiopia. *Journal of African Earth Sciences* 59, 295–312.

Caliro, S., Chiodini, G., Izzo, G., Minopoli, C., Signorini, A., Avino, R., Granieri, D., 2008. Geochemical and biochemical evidence of lake overturn and fish kill at Lake Averno, Italy. *Journal of Volcanology and Geothermal Research* 178, 305–316.

Camberlin, P., 1997. Rainfall anomalies in the source region of the Nile and their connection with the Indian summer monsoon. *Journal of Climate* 10, 1380–1392.

Carignan, J., Hild, P., Mevelle, G., Morel, J., Yeghicheyan, D., 2001. Routine analyses of trace elements in geological samples using flow injection and low pressure on-line liquid chromatography coupled to ICP-MS: a study of geochemical reference materials BR, DR-N, UB-N, AN-G and GH. *Geostandards and Geoanalytical Research* 25, 187–198.

Cerling, T.E., 1979. Palaeochemistry of Plio-Pleistocene Lake Turkana, Kenya. *Palaeogeography, Palaeoclimatology, Palaeoecology* 27, 247–285.

Chorowicz, J., 2005. The east African rift system. *Journal of African Earth Sciences* 43, 379–410.

Cohen, A., 1981. Paleolimnological research at Lake Turkana, Kenya. *Palaeoecology of Africa* 13, 61–82.

Cohen, A.S., 2003. *Palaeolimnology: The History and Evolution of Lake Systems*. Oxford University Press, New York.

Cuthbert, M.O., Gleeson, T., Reynolds, S.C., Bennett, M.R., Newton, A.C., McCormack, C.J., Ashley, G.M., 2017. Modelling the role of groundwater hydro-refugia in East African hominin evolution and dispersal. *Nature Communications* 8, 15696.

Danielson, J.J., Gesch, D.B., 2011. Global Multi-resolution Terrain Elevation Data 2010 (GMTED2010). Open-File Report No. 2011-1073. U.S. Geological Survey, Earth Resources Observation and Science Center, Sioux Falls, SD.

de Heinzelin, J., 1983. The Omo Group: Archives of the International Omo Research Expedition. Annales du Musée Royal de l'Afrique Centrale, série, 8. Musée Royal de l'Afrique Centrale, Tervuren, Belgium.

Deino, A.L., Kingston, J.D., Glen, J.M., Edgar, R.K., Hill, A., 2006. Precessional forcing of lacustrine sedimentation in the late Cenozoic Chemeron Basin, Central Kenya Rift, and calibration of the Gauss/Matuyama boundary. *Earth and Planetary Science Letters* 247, 41–60.

Delagnes, A., Roche, H., 2005. Late Pliocene hominid knapping skills: the case of Lokalalei 2C, West Turkana, Kenya. *Journal of Human Evolution* 48, 435–472.

deMenocal, P.B., 1995. Plio-Pleistocene African climate. *Science* 270, 53–59.

deMenocal, P.B., 2004. African climate change and faunal evolution during the Pliocene–Pleistocene. *Earth and Planetary Science Letters* 220, 3–24.

Dunkelman, T.J., Karson, J.A., Rosendahl, B.R., 1988. Structural style of the Turkana rift, Kenya. *Geology* 16, 258–261.

Feibel, C.S., 1987. Fossil fish nests from the Koobi Fora Formation (Plio-Pleistocene) of northern Kenya. *Journal of Palaeontology* 61, 130–134.

Feibel, C.S., 1994. Freshwater stingrays from the Plio-Pleistocene of the Turkana Basin, Kenya and Ethiopia. *Lethaia* 26, 359–366.

Feibel, C.S., 1997. A terrestrial auxiliary stratotype point and section for the Plio-Pleistocene boundary in the Turkana Basin, East Africa. *Quaternary International* 40, 73–79.

Feibel, C.S., 2003. Stratigraphy and depositional history of the Lothagam sequence. In: Leakey, M.G., Harris, J.M. (Eds.), *Lothagam: The Dawn of Humanity in Eastern Africa*. Columbia University Press, New York, pp. 17–29.

Feibel, C.S., 2011. *A geological history of the Turkana Basin. Evolutionary Anthropology: Issues, News, and Reviews* 20, 206–216.

Feibel, C.S., Brown, F.H., McDougall, I., 1989. Stratigraphic context of fossil hominids from the Omo Group deposits: northern Turkana Basin, Kenya and Ethiopia. *American Journal of Physical Anthropology* 78, 595–622.

Garcin, Y., Melnick, D., Strecker, M.R., Olago, D., Tiercelin, J.J., 2012. East African mid-Holocene wet–dry transition recorded in palaeo-shorelines of Lake Turkana, northern Kenya Rift. *Earth and Planetary Science Letters* 331, 322–334.

Gathogo, P.N., Brown, F.H., McDougall, I., 2008. Stratigraphy of the Koobi Fora Formation (Pliocene and Pleistocene) in the Loiyangalani region of northern Kenya. *Journal of African Earth Sciences* 51, 277–297.

Gupta, A.K., Dhingra, H., Mélice, J.L., Anderson, D.M., 2001. Earth's eccentricity cycles and Indian Summer Monsoon variability over the past 2 million years: evidence from deep-sea benthic foraminifer. *Geophysical Research Letters* 28, 4131–4134.

Gupta, A.K., Thomas, E., 2003. Initiation of Northern Hemisphere glaciation and strengthening of the northeast Indian monsoon: Ocean Drilling Program Site 758, eastern equatorial Indian Ocean. *Geology* 31, 47–50.

Haileab, B., 1995. Geochemistry, Geochronology and Tephrostratigraphy of Tephra from the Turkana Basin, Southern Ethiopia and Northern Kenya. PhD dissertation, University of Utah, Salt Lake City.

Haileab, B., Brown, F.H., McDougall, I., Gathogo, P.N., 2004. Gombe Group basalts and initiation of Pliocene deposition in the Turkana depression, northern Kenya and southern Ethiopia. *Geological Magazine* 141, 41–53.

Halfman, J.D., 1987. High-Resolution Sedimentology and Palaeoclimatology of Lake Turkana, Kenya. PhD dissertation, Duke University, Durham, NC.

Harmand, S., Lewis, J.E., Feibel, C.S., Lepre, C.J., Prat, S., Lenoble, A., Boës, X., et al., 2015. 3.3-Million-year-old stone tools from Lomekwi 3, West Turkana, Kenya. *Nature* 521, 310–315.

Harris, J.M., Brown, F.H., Leakey, M.G., 1988. Stratigraphy and palaeontology of the Nachukui Formation, Lake Turkana region, Kenya. *Contributions in Science*, *Los Angeles County Museum of Natural History* 399, 1–128.

Hillhouse, J.W., Cerling, T.E., Brown, F.H., 1986. Magnetostratigraphy of the Koobi Fora Formation, Lake Turkana, Kenya. *Journal of Geophysical Research: Solid Earth* 91, 11581–11595.

Hillhouse, J.W., Ndombi, J.W.M., Cox, A., Brock, A., 1977. Additional results on palaeomagnetic stratigraphy of the Koobi Fora Formation, east of Lake Turkana (Lake Rudolf), Kenya. *Nature* 265, 411–415.

Joordens, J.C.A., Vonhof, H.B., Feibel, C.S., Lourens, L.J., Dupont-Nivet, G., van der Lubbe, J.H.J.L., Sier, M.J., Davies, G.R., Kroon, D., 2011. An astronomically-tuned climate framework for hominins in the Turkana Basin. *Earth and Planetary Science Letters* 307, 1–8.

Kelts, K., Talbot, M., 1990. Lacustrine carbonates as geochemical archives of environmental change and biotic/abiotic interactions. In: Tilzer, M.M., Serruya, C. (Eds.), *Large Lakes*. Springer, Berlin, pp. 288–315.

Kibunjia, M., 1994. Pliocene archaeological occurrences in the Lake Turkana basin. *Journal of Human Evolution* 27, 159–171.

Kibunjia, M., Roche, H., Brown, F.H., Leakey, R.E., 1992. Pliocene and Pleistocene archeological sites west of Lake Turkana, Kenya. *Journal of Human Evolution* 23, 431–438.

Kingston, J.D., Deino, A.L., Edgar, R.K., Hill, A., 2007. Astronomically forced climate change in the Kenyan Rift Valley 2.7–2.55 Ma: implications for the evolution of early hominin ecosystems. *Journal of Human Evolution* 53, 487–503.

Laskar, J., Robutel, P., Joutel, F., Gastineau, M., Correia, A.C.M., Levrard, B., 2004. A long-term numerical solution for the insolation quantities of the Earth. *Astronomy and Astrophysics* 428, 261–285.

Last, W.M., Smol, J.P. (Eds.), 2006. *Tracking Environmental Change Using Lake Sediments. Vol. 2, Physical and Geochemical Methods*. Springer Science & Business Media, Dordrecht, the Netherlands.

Leakey, M.G., Spoor, F., Brown, F.H., Gathogo, P.N., Kiarie, C., Leakey, L.N., McDougall, I., 2001. New hominin genus from eastern Africa shows diverse middle Pliocene lineages. *Nature* 410, 433–440.

Leakey, R.E.F., Walker, A., 1988. New *Australopithecus boisei* specimens from east and west Lake Turkana, Kenya. *American Journal of Physical Anthropology* 76, 1–24.

https://doi.org/10.1017/qua.2018.118 Published online by Cambridge University Press

Lepre, C.J., 2014. Early Pleistocene lake formation and hominin origins in the Turkana–Omo rift. *Quaternary Science Reviews* 102, 181–191.

Lepre, C.J., Kent, D.V., 2010. New magnetostratigraphy for the Olduvai Subchron in the Koobi Fora Formation, northwest Kenya, with implications for early *Homo*. *Earth and Planetary Science Letters* 290, 362–374.

Lepre, C.J., Roche, H., Kent, D.V., Harmand, S., Quinn, R.L., Brugal, J.P., Texier, P.J., Feibel, C.S., 2011. An earlier origin for the Acheulian. *Nature* 477, 82–85.

Levin, N.E., 2015. Environment and climate of early human evolution. *Annual Review of Earth and Planetary Sciences* 43, 405–429.

Lewis, J.E., Harmand, S., 2016. An earlier origin for stone tool making: implications for cognitive evolution and the transition to *Homo*. *Philosophical Transactions of the Royal Society B: Biological Sciences* 371, 20150233.

Lien, L., Liti, D., Kallqvist, T., 1988. *Lake Turkana Limnological Study 1985-1988*. Norwegian Institute for Water Research, Oslo.

Lisiecki, L.E., 2010. Links between eccentricity forcing and the 100,000-year glacial cycle. *Nature Geoscience* 3, 349–352.

Maslin, M.A., Brierley, C.M., Milner, A.M., Shultz, S., Trauth, M. H., Wilson, K.E., 2014. East African climate pulses and early human evolution. *Quaternary Science Reviews* 101, 1–17.

Maslin, M.A., Shultz, S., Trauth, M.H., 2015. A synthesis of the theories and concepts of early human evolution. *Philosophical Transactions of the Royal Society B: Biological Sciences* 370, 20140064.

McDougall, I., Brown, F.H., 2008. Geochronology of the pre-KBS Tuff sequence, Omo Group, Turkana Basin. *Journal of the Geological Society* 165, 549–562.

McDougall, I., Brown, F.H., Vasconcelos, P.M., Cohen, B.E., Thiede, D.S., Buchanan, M.J., 2012. New single crystal 40Ar/39Ar ages improve time scale for deposition of the Omo Group, Omo–Turkana Basin, East Africa. *Journal of the Geological Society* 169, 213–226.

McGrath, M., Davison, W., Hamilton-Taylor, J., 1989. Biogeochemistry of barium and strontium in a softwater lake. *Science of the Total Environment* 87, 287–295.

Merlis, T.M., Schneider, T., Bordoni, S., Eisenman, I., 2013. The tropical precipitation response to orbital precession. *Journal of Climate* 26, 2010–2021.

Nicholson, S.E., 1996. A review of climate dynamics and climate variability in eastern Africa. In: Johnson, T.C., Odada, E.O. (Eds.), *The Limnology, Climatology and Paleoclimatology of the East African Lakes*. Gordon and Breach, Amsterdam, pp. 25–56.

Nicholson, S.E., 2009. A revised picture of the structure of the "monsoon" and land ITCZ over West Africa. *Climate Dynamics* 32, 1155–1171.

Nicholson, S.E., 2016. The Turkana low-level jet: mean climatology and association with regional aridity. *International Journal of Climatology* 36, 2598–2614.

Nutz, A., Schuster, M., Boës, X., Rubino, J.L., 2017. Orbitally-driven evolution of Lake Turkana (Turkana Depression, Kenya, EARS) between 1.95 and 1.72 Ma: a sequence stratigraphy perspective. *Journal of African Earth Sciences* 125, 230–243.

Olago, D., Odada, E., 1996. Some aspects of the physical and chemical dynamics of a large rift lake: the Lake Turkana north basin, northwest Kenya. In: Johnson, T.C., Odada, E.O. (Eds.), *The Limnology, Climatology and Palaeoclimatology of the East African Lakes*. Gordon and Breach, Amsterdam, pp. 413–430.

Olaka, L.A., Odada, E.O., Trauth, M.H., Olago, D.O., 2010. The sensitivity of East African rift lakes to climate fluctuations. *Journal of Paleolimnology* 44, 629–644.

Opdyke, N.D., Kent, D.V., Huang, K., Foster, D.A., Patel, J.P., 2010. Equatorial paleomagnetic time-averaged field results from 0–5 Ma lavas from Kenya and the latitudinal variation of angular dispersion. *Geochemistry, Geophysics, Geosystems* 11, Q05005.

Passey, B.H., Levin, N.E., Cerling, T.E., Brown, F.H., Eiler, J.M., 2010. High-temperature environments of human evolution in East Africa based on bond ordering in paleosol carbonates. *Proceedings of the National Academy of Sciences of the United States of America* 107, 11245–11249.

Peel, M.C., Finlayson, B.L., McMahon, T.A., 2007. Updated world map of the Köppen-Geiger climate classification. *Hydrology and Earth System Sciences Discussions* 4, 439–473.

Peinerud, E.K., Ingri, J., Pontér, C., 2001. Non-detrital Si concentrations as an estimate of diatom concentrations in lake sediments and suspended material. *Chemical Geology* 177, 229–239.

Prat, S., Brugal, J.P., Roche, H., Texier, P.J., 2003. Nouvelles découvertes de dents d'hominidés dans le membre Kaitio de la formation de Nachukui (1,65–1,9 Ma), Ouest du lac Turkana (Kenya). *Comptes Rendus Palevol* 2, 685–693.

Prat, S., Brugal, J.P., Tiercelin, J.J., Barrat, J.A., Bohn, M., Delagnes, A., Harmand, S., *et al.*, 2005. First occurrence of early *Homo* in the Nachukui Formation (West Turkana, Kenya) at 2.3-2.4 Myr. *Journal of Human Evolution* 49, 230–240.

Quidelleur, X., Holt, J.W., Salvany, T., Bouquerel, H., 2010. New K-Ar ages from La Montagne massif, Réunion Island (Indian Ocean), supporting two geomagnetic events in the time period 2.2–2.0 Ma. *Geophysical Journal International* 182, 699–710.

Raymo, M.E., Hodell, D., Jansen, E., 1992. Response of deep ocean circulation to initiation of Northern Hemisphere glaciation (3–2 Ma). *Paleoceanography* 7, 645–672.

Roche, H., Brugal, J.P., Delagnes, A., Feibel, C., Harmand, S., Kibunjia, M., Prat, S., Texier, P.J., 2003. Les sites archéologiques plio-pléistocènes de la formation de Nachukui, Ouest-Turkana, Kenya: bilan synthétique 1997–2001. *Comptes Rendus Palevol* 2, 663–673.

Roche, H., Delagnes, A., Brugal, J.P., Feibel, C., Kibunjia, M., Mourre, V., Texier, P.J., 1999. Early hominid stone tool production and technical skill 2.34 Ma ago in West Turkana, Kenya. *Nature* 399, 57–60.

Roche, H., de la Torre, I., Arroyo, A., Brugal, J.P., Harmand, S., 2018. Naiyena Engol 2 (West Turkana, Kenya): a case study on variability in the Oldowan. *African Archaeological Review* 35, 57–85.

Roman, D., Campisano, C., Quade, J., DiMaggio, E., Arrowsmith, R., Feibel, C., 2008. Composite tephrostratigraphy of the Dikika, Gona, Hadar, and Ledi-Geraru project areas, northern Awash, Ethiopia. In: Quade, J., Wynn, J.G. (Eds.), *The Geology of Early Humans in the Horn of Africa*. Geological Society of America, Special Paper 446, 119–134.

Rossignol-Strick, M., 1983. African monsoons, an immediate climate response to orbital insolation. *Nature* 304, 46–49.

Schuster, M., Nutz, A., 2018. Lacustrine wave-dominated clastic shorelines: modern to ancient littoral landforms and deposits from the Lake Turkana Basin (East African Rift System, Kenya). *Journal of Palaeolimnology* 59, 221–243.

Sepulchre, P., Ramstein, G., Fluteau, F., Schuster, M., Tiercelin, J.J., Brunet, M., 2006. Tectonic uplift and eastern Africa aridification. *Science* 313, 1419–1423.

https://doi.org/10.1017/qua.2018.118 Published online by Cambridge University Press

Singer, B.S., Jicha, B.R., Condon, D.J., Macho, A.S., Hoffman, K.A., Dierkhising, J., Brown, M.C., Feinberg, J.M., Kidane, T., 2014. Precise ages of the Réunion event and Huckleberry Ridge excursion: episodic clustering of geomagnetic instabilities and the dynamics of flow within the outer core. *Earth and Planetary Science Letters* 405, 25–38.

Tiercelin, J.J., Schuster, M., Roche, H., Brugal, J.P., Thuo, P., Prat, S., Harmand, S., Gourguen, D., Barrat, J.A., Bohn, M., 2010. New considerations on the stratigraphy and environmental context of the oldest (2.34 Ma) Lokalalei archaeological site complex of the Nachukui Formation, West Turkana, northern Kenya Rift. *Journal of African Earth Sciences* 58, 157–184.

Trauth, M.H., Maslin, M.A., Deino, A., Strecker, M.R., 2005. Late Cenozoic moisture history of East Africa. *Science* 309, 2051–2053.

Trauth, M.H., Maslin, M.A., Deino, A.L., Junginger, A., Lesoloyia, M., Odada, E.O., Olago, D.O., Olaka, L.A., Strecker, M.R., Tiedemann, R., 2010. Human evolution in a variable environment: the amplifier lakes of Eastern Africa. *Quaternary Science Reviews* 29, 2981–2988.

Trauth, M.H., Maslin, M.A., Deino, A.L., Strecker, M.R., Bergner, A.G., Dühnforth, M., 2007. High-and low-latitude forcing of Plio-Pleistocene East African climate and human evolution. *Journal of Human Evolution* 53, 475–486.

Volkova, N.I., 1998. Geochemistry of rare elements in waters and sediments of alkaline lakes in the Sasykkul depression, East Pamirs. *Chemical Geology* 147, 265–277.

Vonhof, H.B., Joordens, J.C., Noback, M.L., van der Lubbe, J.H., Feibel, C.S., Kroon, D., 2013. Environmental and climatic control on seasonal stable isotope variation of freshwater molluscan bivalves in the Turkana Basin (Kenya). *Palaeogeography, Palaeoclimatology, Palaeoecology* 383, 16–26.

Walker, A., Leakey, R.E., 1993. *The Nariokotome Homo erectus Skeleton*. Harvard University Press, Cambridge, MA.

Walker, A., Leakey, R.E., Harris, J.M., Brown, F.H., 1986. 2.5-Ma *Australopithecus boisei* from west of Lake Turkana, Kenya. *Nature* 322, 517–522.

Watkins, R.T., 1986. Volcano-tectonic control on sedimentation in the Koobi Fora sedimentary basin, Lake Turkana. *Geological Society, London, Special Publications* 25, 85–95.

Williamson, P.G., 1982. Molluscan biostratigraphy of the Koobi Fora hominid–bearing deposits. *Nature* 295, 140–142.

Wood, B., Constantino, P., 2007. *Paranthropus boisei*: fifty years of evidence and analysis. *American Journal of Physical Anthropology* 134, 106–132.

Wood, B., Leakey, M., 2011. The Omo-Turkana Basin fossil hominins and their contribution to our understanding of human evolution in Africa. *Evolutionary Anthropology: Issues, News, and Reviews* 20, 264–292.

Yan, J.P., Hinderer, M., Einsele, G., 2002. Geochemical evolution of closed-basin lakes: general model and application to Lakes Qinghai and Turkana. *Sedimentary Geology* 148, 105–122.

Yuretich, R.F., Cerling, T.E., 1983. Hydrogeochemistry of Lake Turkana, Kenya: mass balance and mineral reactions in an alkaline lake. *Geochimica et Cosmochimica Acta* 47, 1099–1109.

https://doi.org/10.1017/qua.2018.118 Published online by Cambridge University Press